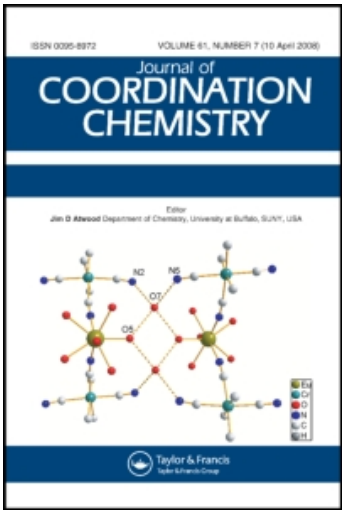

Journal of Coordination Chemistry
Publication details, including instructions for authors and subscription information:
http://www.informaworld.com/smpp/title~content=t713455674

Formation of $[FeW_{12}O_{40}]^{5-}$ under hydrothermal conditions: syntheses, crystal structures, and characterization of $[Fe(2,2'\text{-bipy})_3]_2[HFeW_{12}O_{40}] \cdot 5H_2O$ and $(4,4'\text{-}H_2bipy)_6(Hpy)_2(H_3O)[FeW_{12}O_{40}]_3 \cdot 11H_2O$

Jia Li[a]; Ya-Guang Chen[a]; Chun-Jing Zhang[a]
[a] Key Laboratory of Polyoxometalate Science of Ministry of Education, College of Chemistry, Northeast Normal University, Changchun 130024, PRC

To cite this Article Li, Jia , Chen, Ya-Guang and Zhang, Chun-Jing(2009) 'Formation of $[FeW_{12}O_{40}]^{5-}$ under hydrothermal conditions: syntheses, crystal structures, and characterization of $[Fe(2,2'\text{-bipy})_3]_2[HFeW_{12}O_{40}] \cdot 5H_2O$ and $(4,4'\text{-}H_2bipy)_6(Hpy)_2(H_3O)[FeW_{12}O_{40}]_3 \cdot 11H_2O$', Journal of Coordination Chemistry, 62: 23, 3810 — 3818
To link to this Article: DOI: 10.1080/00958970903177489
URL: http://dx.doi.org/10.1080/00958970903177489

Journal of Coordination Chemistry
Vol. 62, No. 23, 10 December 2009, 3810–3818

Taylor & Francis
Taylor & Francis Group

Formation of $[FeW_{12}O_{40}]^{5-}$ under hydrothermal conditions: syntheses, crystal structures, and characterization of $[Fe(2,2'\text{-bipy})_3]_2[HFeW_{12}O_{40}]\cdot 5H_2O$ and $(4,4'\text{-}H_2bipy)_6(Hpy)_2(H_3O)[FeW_{12}O_{40}]_3\cdot 11H_2O$

JIA LI, YA-GUANG CHEN* and CHUN-JING ZHANG

Key Laboratory of Polyoxometalate Science of Ministry of Education, College of Chemistry, Northeast Normal University, Changchun 130024, PRC

(*Received 8 April 2009; in final form 1 June 2009*)

Two supramolecular compounds based on tungstoferrate $[FeW_{12}O_{40}]^{5-}$, $[Fe^{II}(2,2'\text{-bipy})_3]_2[HFeW_{12}O_{40}]\cdot 5H_2O$ (**1**), and $[Hpy]_2[4,4'\text{-}H_2bipy]_6(H_3O)[FeW_{12}O_{40}]_3\cdot 11H_2O$ (**2**) (py = pyridine, bipy = bipyridine) were synthesized hydrothermally and characterized structurally. The hydrogen bonds between polyoxoanions and water and the edge-to-face π–π interaction between $[Fe^{II}(2,2'\text{-bipy})_3]^{2+}$ with a shortest C–C distance of 3.513 Å are the main forces to construct the 3-D architecture of **1**. In **2**, a 3-D supramolecular architecture is assembled by the tungstoferrate anions, protonated 4,4′-bipy cations, and water through hydrogen bonding. The variable-temperature magnetic susceptibilities indicate that **1** is paramagnetic with μ_{eff} corresponding to one Fe(III) with spin-only contribution, showing that Fe in the coordination cations has a +II oxidation number and low spin state.

Keywords: Tungstoferrate; Hydrothermal synthesis; Hydrogen bond; Iron; Crystal structure

1. Introduction

Organic–inorganic hybrids based on polyoxometalates (POMs) as inorganic building blocks have attracted more attention due to diverse topologic structures and potential applications [1]. Interactions in the organic–inorganic hybrids include electrostatic forces, van der Waals forces, hydrogen bonds, and π–π stacking. Combination of organic and inorganic components may bring hybrids with new functions and properties [2]. POMs as inorganic building blocks have high negative charges and many surface oxygens, which are able to coordinate to transition metals in many modes, and also act as acceptors of hydrogen bonds. There are many reports about these hybrids containing POMs [3, 4], including 15 articles about organic–inorganic hybrids based on POMs published in [5]; these reports are based on hetero-POMs with main group elements as central atom or homo-POMs, but there are a few hybrids containing iron atoms [4] either as components of POM or as metal-organic motifs.

*Corresponding author. Email: chenyg146@nenu.edu.cn

Journal of Coordination Chemistry
ISSN 0095-8972 print/ISSN 1029-0389 online
DOI: 10.1080/00958970903177489

Heteropolyanions containing main-group elements such as phosphorus or silicon as the central atom could be prepared easily in a relatively high yield, but those containing transition metal elements, e.g., Cr, Fe, and Cu, as the central atom can only be obtained in low yield. Their formation is commonly accompanied with paratungstate as the by-product. In 1950, Mair [6] first reported $[FeW_{12}O_{40}]^{5-}$ and later Pope and Varga [7] modified the synthesis of $[FeW_{12}O_{40}]^{5-}$; there is no further modification in the synthesis of $[FeW_{12}O_{40}]^{5-}$. The low yield of $[FeW_{12}O_{40}]^{5-}$ may arise from the large size of Fe(III) compared to P(V) or Si(IV), which reduces the combination between W_3O_{13} tri-metal clusters. During our research on organic–inorganic hybrids based on POM, we found that $[FeW_{12}O_{40}]^{5-}$ could be formed under hydrothermal conditions [8]. Herein we give the syntheses, crystal structures, and characterization of two new supramolecular compounds of tungstoferrates, $[Fe(2,2\text{-bipy})_3]_2[HFeW_{12}O_{40}]\cdot 5H_2O$ (**1**), and $[Hpy]_2[4,4\text{-}H_2bipy]_6(H_3O)[FeW_{12}O_{40}]_3\cdot 11H_2O$ (**2**) (py = pyridine, bipy = bipyridine).

2. Experimental

2.1. *General procedures*

All reagents of analytical grade were obtained from commercial sources and used without purification. Elemental analyses (C, H, and N) were performed on a Perkin–Elmer 2400 CHN Elemental Analyzer. W and Fe were determined by a Leaman inductively coupled plasma (ICP) spectrometer. IR spectra were obtained in the range of 400–4000 cm^{-1} on an Alpha Centauri FT/IR spectrophotometer using KBr pellets. TG analysis was performed on a Perkin–Elmer TGA7 instrument in flowing N_2 with a heating rate of 10°C min^{-1}. Magnetic properties were performed on crystalline samples with a Quantum Design MPMS-5SQUID magnetometer in the range of 2–300 K.

2.2. *Hydrothermal syntheses*

2.2.1. Synthesis of $[Fe(2,2'\text{-bipy})_3]_2[HFeW_{12}O_{40}]\cdot 5H_2O$ (1). A mixture of $Na_2WO_4\cdot 2H_2O$ (0.6 g), $Fe(NO_3)_3\cdot 9H_2O$ (0.094 g), 2,2′-bipy (0.04 g), and H_2O (15 mL) was stirred for 20 min in air. The pH was adjusted to 4.3 by the addition of 1 mol L^{-1} HCl aqueous solution. The final solution was then transferred to a 20 mL Teflon-lined autoclave and kept at 165°C for 4 days. The autoclave was cooled at 10°C h^{-1} to room temperature and the resulting red-block crystals were filtered off, washed with distilled water, and dried at ambient temperature. Elemental analytical results of crystals are consistent with the stoichiometry of **1** (30% yield based on W). Anal. Calcd for $C_{60}H_{59}Fe_3N_{12}O_{45}W_{12}$ (4041.92) (%): C, 17.83; H, 1.47; N, 4.16; Fe, 4.15; W, 54.58. Found (%): C, 17.80; H, 1.55; N, 4.17; Fe, 4.19; W, 54.29.

2.2.2. Synthesis of $[Hpy]_2[4,4'\text{-}H_2bipy]_6(H_3O)[FeW_{12}O_{40}]_3\cdot 11H_2O$ (2). A mixture of $Na_2WO_4\cdot 2H_2O$ (0.6 g), $Fe(NO_3)_3\cdot 9H_2O$ (0.104 g), 4,4′-bipy (0.039 g), and 12 mL water was stirred for 20 min in air. The pH was adjusted to 2.1 by the addition of 1 mol L^{-1} HCl aqueous solution. The final solution was then transferred to a 20 mL Teflon-lined autoclave and kept at 165°C for 4 days. The autoclave was cooled at 10°C h^{-1} to

room temperature. The resulting orange block crystals were filtered off, washed with distilled water, and dried at ambient temperature. Elemental analytical results of crystals are consistent with the stoichiometry of **2** (35% yield based on W). Anal. Calcd for $C_{70}H_{97}Fe_3N_{14}O_{132}W_{36}$ (10032.69) (%): C, 8.38; H, 0.97; N, 1.95; Fe, 1.67; W, 65.97. Found (%): C, 8.41; H, 1.11; N, 2.01; Fe, 1.76; W, 64.79.

2.3. *X-ray crystallography*

Single-crystal X-ray diffraction data of **1** and **2** were collected on a Bruker Smart Apex CCD diffractometer at 293 K using graphite-monochromated Mo-Kα radiation ($\alpha = 0.71069$ Å) and omega scans technique; an empirical absorption correction was applied. The structures were solved by direct methods and refined by full-matrix least-squares on F^2 with SHELXL-97 software [9]. All non-hydrogen atoms were refined anisotropically. Hydrogens on carbons were positioned geometrically and refined as riding atoms with d(C–H) = 0.93 Å and U_{iso}(H) = 1.2U_{eq}(C). Hydrogens of disordered waters were not located. Further details of crystallographic data and structural determination of **1** and **2** are given in table 1. Selected bond lengths and angles of **1** and **2** are listed in tables S1 and S2.

Table 1. Crystal data and structure refinement of **1** and **2**.

Compound	**1**	**2**
Empirical formula	$C_{60}H_{58}Fe_3N_{12}O_{45}W_{12}$	$C_{70}H_{97}Fe_3N_{14}O_{132}W_{36}$
Formula weight	4041.92	10031.4
Crystal system	Triclinic	Triclinic
Space group	*P*-1	*P*-1
Unit cell dimensions (Å, °)		
a	13.910(5)	11.882(5)
b	17.881(5)	19.255(5)
c	19.028(5)	21.067(5)
α	88.146(5)	63.506(5)
β	72.356(5)	73.899(5)
γ	74.849(5)	79.580(5)
Volume (Å^3), *Z*	4348(2), 2	4135(2), 1
Calculated density (g cm^{-3})	3.101	4.029
F(000)	3678	4412
Limiting indices	$-15 \le h \le 17$; $-16 \le k \le 21$; $-21 \le l \le 23$	$-15 \le h \le 15$; $-24 \le k \le 25$; $-27 \le l \le 28$
Absorption coefficient (mm^{-1})	16.384	25.284
Absorption correction	Empirical	Empirical
θ range for data collection (°)	1.59–25.75	1.18–28.36
Reflections collected	23,541	20,688
Independent reflections	16,622 [R(int) = 0.0338]	18,486 [R(int) = 0.0369]
Data/restraints/parameters	16318/0/1220	18486/541/1155
Goodness-of-fit on F^2	0.995	1.026
Final R indices [$I > 2\sigma(I)$]	$R_1 = 0.0424$, $wR_2 = 0.1023$	$R_1 = 0.0671$, $wR_2 = 0.1502$
R indices (all data)	$R_1 = 0.0632$, $wR_2 = 0.1102$	$R_1 = 0.1017$, $wR_2 = 0.1664$
Extinction coefficient	0.000144(15)	0.000121(11)
Largest difference peak and hole (e Å^{-3})	2.890 and −2.240	4.460 and −4.247

3. Results and discussion

3.1. *Formation of the compounds*

Two compounds were obtained under almost identical conditions except for isomeric ligands and the pH values of the reaction solution, showing that tungstoferrate(III) anion could be formed in a pH range of 2.1–4.3 under hydrothermal conditions, different conditions from that reported earlier [6, 7]. This result provides a new way to obtain tungstoferrate anion. Using chelating 2,2′-bipy resulted in a coordination cation as counterion and the nitrogens did not take part in the formation of hydrogen bonds; using bridging 4,4′-bipy gave the protonated organic cation as counterion and donor of hydrogen bonds. The pH of reaction solution also exerts an important influence in the formation of **1** and **2**. The relatively low pH leads to the competition of hydrogen and iron ions to ligands and does not favor the formation of coordination cation; at pH higher than 2.1 there are no crystalline species in the synthesis of **2**, showing that the relative low pH value favored the protonation of 4,4′-bipy and crystallization of **2**. At pH lower than 4.3, **1** could not be obtained due to the protonation of 2,2′-bipy. We had the same experience using 1,10-phenanthroline [8]. Some 4,4′-bipy split into pyridine in the synthesis of **2**. Organic ligands changing into other molecules under hydrothermal conditions have been reported [10].

3.2. *Crystal structure description*

The single-crystal X-ray structure analysis reveals that **1** consists of one discrete anion $[HFeW_{12}O_{40}]^{4-}$, two $[Fe(2,2'\text{-bipy})_3]^{2+}$, and five waters (figure 1). The anion has a classic Keggin structure (general formula $[XM_{12}O_{40}]^{n-}$). The central Fe exhibits FeO_4 tetrahedral geometry, with Fe–O distances of 1.815(7)–1.840(8) Å and the peripheral W atoms exhibit $\{WO_6\}$ octahedral configuration. Three $\{MO_6\}$ octahedra constitute a tri-metal cluster, and the tri-metal clusters arrange tetrahedrally around the FeO_4 tetrahedron. The W–O distances are in the range of 1.695(8)–1.730(9) Å for W–O_d bonds, 1.871(8)–1.991(7) Å for W–$O_{b,c}$ bonds, and 2.191(7)–2.242(7) Å for W–O_a bonds, consistent with the reported values [11]. In $[Fe(2,2\text{-bipy})_3]^{2+}$, Fe^{2+} is coordinated by six nitrogens from three 2,2′-bipy molecules with Fe–N distances of 1.951(11)–1.976(10) Å and N–Fe–N bond angles of 81.0(4)°–176.6(4)°, showing a slightly distorted octahedral geometry.

In the crystals there exist many hydrogen bonds between the anions and lattice waters (table 2). In [011] direction two pairs of hydrogen bonds (O21–O3W–O2W–O7# and O21#–O3W–O2W–O7) link two anions, and in *a*-axis direction O1W links two anions via hydrogen chain (O6–O1W–O9#), forming a ladder chain structure. These chains create a layer structure through hydrogen bonds of O5W and O4W. That is, the anion acts as the hydrogen bond acceptor forming a 2-D hydrogen bond network. Between layers there is another type of hydrogen bond, C–H···O (C18H18A···O31, C7H O31, C16H O22, C25H O3, C33H O18, C45H O1) with C–O distances of 3.364 Å–3.232, 3.289, 3.063, 3.342, 3.148; ∠CHO 156.0°, 135.9°, 131.0°, 131.25°, 129.5°, and 150.0°, respectively.

In addition, between the cations $[Fe(2,2'\text{-bipy})_3]^{2+}$ there exist edge-to-face π–π interactions with a shortest C–C distance of 3.513 Å (figure 2). Thus, besides the

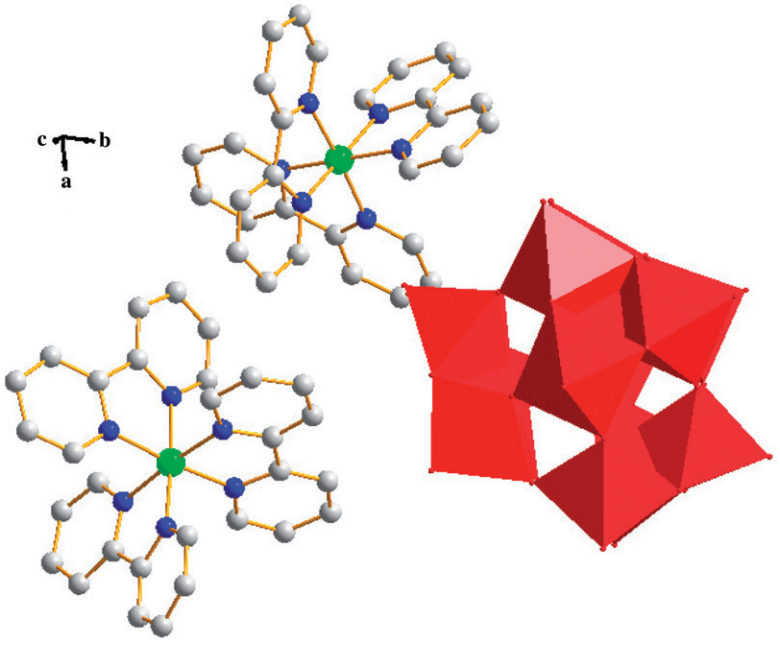

Figure 1. Molecular structure of **1**. All hydrogens and solvent waters are omitted for clarity.

Table 2. Hydrogen bonds with H···A < r(A) + 2.000 Å and ∠DHA > 110° in **1** and **2**.

D–H	d(H···A)	DHA	d(D···A)	A
1				
O1W–H11B	2.147	168.42	3.094	O9 [x–1, y, z]
O1W–H11C	2.209	178.84	3.060	O6
O2W–H11E	1.918	177.95	2.767	O7
O2W–H11F	2.094	178.46	2.943	O3W [$-x+2, -y, -z+1$]
O3W–H10B	2.150	132.86	2.891	O21
O3W–H10C	2.173	136.33	2.943	O2W [$-x+2, -y, z+1$]
O5W–H10D	2.472	111.98	2.968	O25 [$-x+1, -y+1, -z+1$]
O5W–H10E	1.950	162.15	2.878	O4W
2				
O1W–H11L	2.246	142.63	3.064	O2W [$x, y, z-1$]
O2W–H11I	2.094	160.46	3.016	O48 [$x, y, z+1$]
O2W–H11J	2.368	129.02	3.064	O1W [$x, y, z+1$]
O3W–H11B		173	3.075	O29 [$-x+2, -y+2, -z+1$]
O3W–H11F	2.211	143.73	3.038	O57 [$x, y+1, z$]
O4W–H11C	2.103	160.62	3.025	O54A [$-x+1, -y+2, -z$]
O6W–H11P	2.306	130.64	3.021	O19 [$-x+1, -y+2, -z$]
N1–H1B	2.238	142.40	2.966	O2
N1–H1B	2.267	136.09	2.948	O58 [$-x+1, -y+2, -z+1$]
N1–H1B	2.379	124.73	2.954	O2A
N2–H2B	2.135	152.86	2.927	O46
N2–H2B	2.470	126.22	3.058	O38
N4–H4B	1.845	168.58	2.693	O3W
N3–H3A	1.846	167.38	2.692	O2W
N5–H5A	2.011	152.65	2.803	O42 [$-x+2, -y+2, -z$]
N6–H6B	1.832	169.39	2.682	O5W
N7–H7B	2.056	161.32	2.884	O35

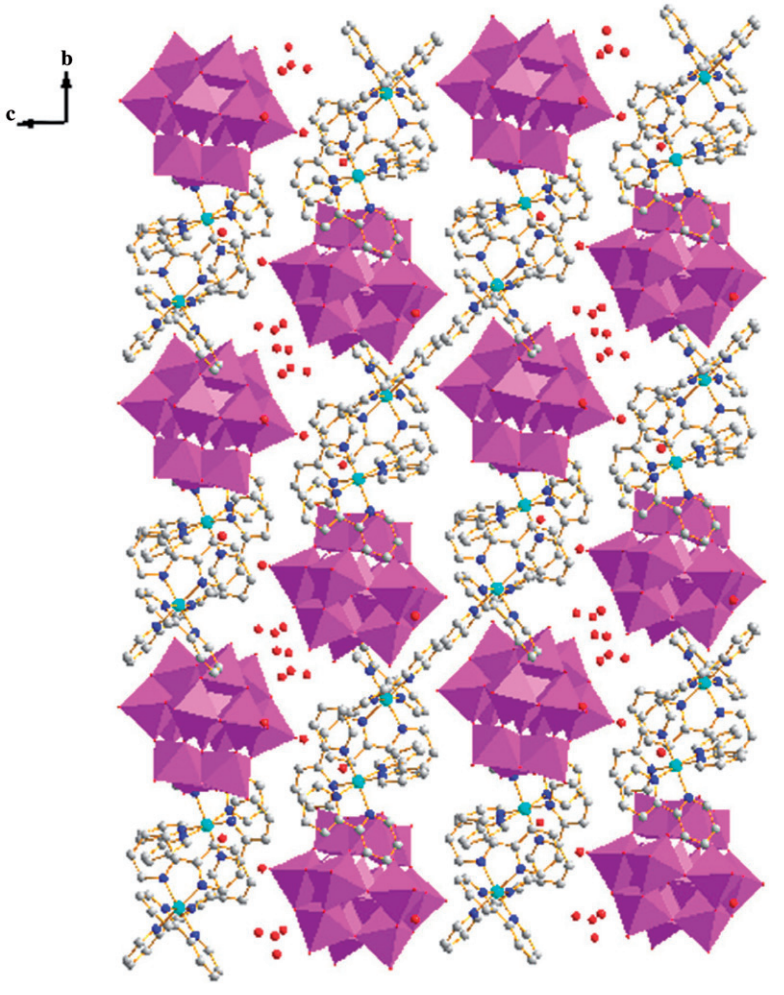

Figure 2. Packing diagram of **1** viewed from the *a*-axis.

electrostatic force between cations and anions, hydrogen bond and π–π interactions play an important role in the crystal structure.

The asymmetric unit of **2** consists of 1.5 $[FeW_{12}O_{40}]^{5-}$ anions, three bi-protonated cations 4,4′-H_2bipy^{2+}, one protonated cation Hpy^{+}, and six waters (figure 3). The $[FeW_{12}O_{40}]^{5-}$ anion in **2** is identical with that in **1** except that one $[FeW_{12}O_{40}]^{5-}$ is orientationally disordered so that there are eight inner oxygens, each of which has half-site occupancy. From the data in table S2, W–O distances vary in a normal range and are consistent with the literature [11]. In the protonated organic cations two pyridine rings are not coplanar with dihedral angles of 18.94°, 28.19°, and 38.51°.

Figure 4 shows the space stacking of **2** viewed from the crystallographic *a*-axis. The formation of hydrogen bonds occurred between bridging and terminal oxygens of the polyoxoanions and waters, protonated bipy and water as well as between water molecules (table 2). Hydrogen bonds link the organic and inorganic motifs, constructing a 3-D architecture of **2**.

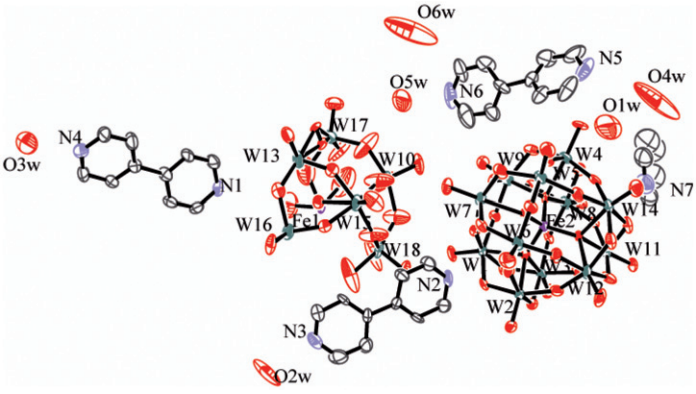

Figure 3. ORTEP drawing (thermal ellipsoids at 50% probability level) of the asymmetric unit of **2**. All hydrogen atoms are omitted for clarity.

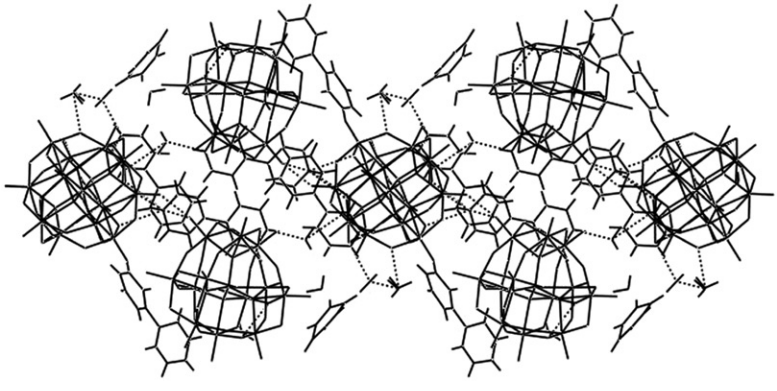

Figure 4. Packing diagram of **2** viewed from the *a*-axis.

3.3. *IR spectrum and thermal analyses*

The IR spectra of **1** and **2** are shown in figures S1 and S2. Characteristic absorptions of $[\alpha\text{-FeW}_{12}O_{40}]^{5-}$ from 1100 to 400 cm^{-1} are observed: 943 and 953 cm^{-1} associated with $\nu_{as}(W{=}O_d)$, 866 and 871 cm^{-1} correspond to $\nu_{as}(W{-}O_c{-}W)$, and 764 cm^{-1} and 763 cm^{-1} are attributed to $\nu_{as}(W{-}O_b{-}W)$ of **1** and **2**, respectively. The absorptions of Fe–O were also observed at 442 and 440 cm^{-1}. In addition, a set of peaks at 1239, 1341, 1443, and 1604 cm^{-1} are characteristic for 2,2′-bipy for **1**. Characteristic bands of 4,4′-bipy for **2** are observed: 1622 cm^{-1} associated with the ring stretching of 4,4′-bipy, 1486 cm^{-1} corresponds to ν_{as}(C–C), and 1205 cm^{-1} corresponds to ν_{as}(C–H). Broad bands of **1** and **2** centered at 3457 and 3437 cm^{-1} result from the vibration of the O–H bonds of H_2O, H–O···H, and N···H–O. Comparing the IR spectra of **1** and **2** with that of $H_5[\alpha\text{-FeW}_{12}O_{40}]$ [12], the vibration frequencies of W–O bonds have shift to lower wavenumbers, showing the interaction of the polyoxoanions and cations as well as water.

In the TG curve of **1** (figure S3), a weight loss of 2.21% (calculated 2.22%) occurs below 130°C, which attributed to the loss of crystal water. The weight loss of 23.23%

(calculated 23.62%) between 380°C and 674°C is ascribed to the release of organic molecules. The wide temperature range implies complicated reactions. In the TG curve of **2** (figure S4), the weight loss of 2.26% at 48–365°C is attributed to the loss of water (Calcd 2.15% for $12H_2O$). From 370°C to 726°C, the weight loss of 11.32% is assigned to the release and decomposition of the organic molecules. The total weight loss of 14.78% at 914°C is bigger than the calculated value of 13.38% for the formula $C_{70}H_{97}Fe_3N_{14}O_{132}W_{36}$ and did not achieve a constant weight at 914°C, which indicates that the thermal decomposition of **2** might include an oxidation–reduction process and the reduction of W(VI) leads to more weight loss. The TG analyses for **1** and **2** support their chemical composition.

3.4. *Magnetism*

The variable-temperature magnetic behavior at a fixed field strength of 1000 Oe for **1** is shown in figure 5 as χ_m *versus* T and $1/\chi_m$ *versus* T curves. As the temperature decreases, the χ_m value increases from 0.017 $cm^3\,mol^{-1}$ at 300 K to a maximum of 2.10 $cm^3\,mol^{-1}$ at about 2 K, and that $1/\chi_m$ *versus* T curve is nearly linear. At 300 K, the effective magnetic moment (μ_{eff}) of 6.39 μ_B is calculated from the formula $\mu_{eff} = 2.828(\chi_m T)^{1/2}$, a little higher than that expected for one high-spin Fe(III) ion (5.92 μ_B) supposing the $g = 2.0$ and higher than that reported [13]. The magnetism indicates that iron in the coordination cations have a +II oxidation number, are in a low spin state and the central Fe is +III oxidation state, supporting the above-given formula.

Supplementary material

Additional information on **1** and **2**, IR spectra, TG graphs, and selected bond lengths and bond angles are given as the supporting information. Crystallographic data have been deposited in the Cambridge Crystallographic Center with CCDC reference

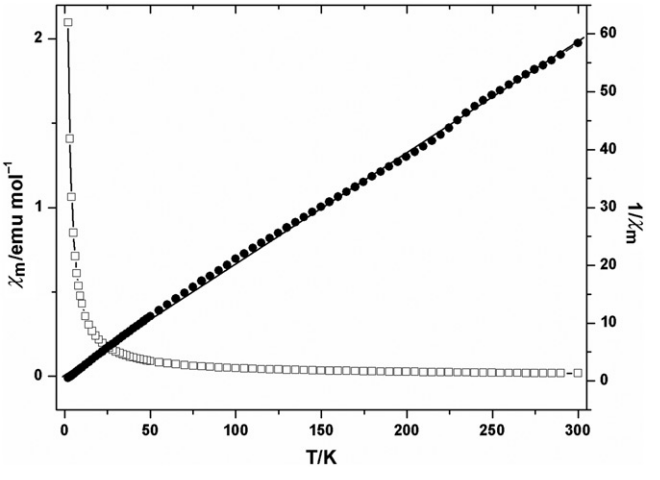

Figure 5. $\chi_m T$ and $1/\chi_m T$ curves of **1**.

numbers: 666135 for **1** and 676698 for **2**. These data can be obtained free of charge via www.ccdc.cam.ac.uk/data_request/cif (Fax: +44-1223-336-033; Email: deposit@ccdc.cam.ac.uk).

Acknowledgment

This work was supported by Analysis and Testing Foundation of the Northeast Normal University.

References

[1] E. Coronado, C.J. Gomez-Garcia. *Chem. Rev*., **98**, 273 (1998).
[2] (a) E. Coronado, C. Giménez-Saiz, C.J. Gómez-García. *Coord. Chem. Rev*., **249**, 1776 (2005); (b) S. Uchida, R. Kawamoto, N. Mizuno. *Inorg. Chem*., **45**, 5136 (2006).
[3] There are a lot of reports about organic–inorganic hybrids based on polyoxometalates, for example: (a) C. Inman, J.M. Knaust, S.W. Keller. *Chem. Commun*., 156–157 (2002); (b) H. Zhang, L.Y. Duan, Y. Lan. *Inorg. Chem*., **42**, 8053 (2003); (c) J.M. Knaust, C. Inman, S.W. Keller. *Chem. Commun*., 492 (2004); (d) Y.P. Ren, X.J. Kong, X.Y. Hu. *Inorg. Chem*., **45**, 4016 (2006); (e) S. Lu, Y.-G. Chen, D.-M. Shi, H.-J. Pang. *Inorg. Chim. Acta*, **361**, 2343 (2008); (f) H. Pang, C. Zhang, D. Shi, Y. Chen. *Cryst. Growth Des*., **8**, 4477 (2008); (g) A.X. Tian, J. Ying, J. Peng. *Inorg. Chem*., **48**, 100 (2009).
[4] (a) Y.-B. Liu, L.-M. Duan, X.-M. Yang, J.-Q. Xu, Q.-B. Zhang, Y.-K. Lu, J. Liu. *J. Solid State Chem*., **179**, 122 (2006); (b) M.-X. Li, H.-Y. Niu, W. Wang, J.-P. Wang. *Z. Naturforsch*., **63b**, 183 (2008); (c) L.-J. Song, H.-Y. Zeng, Z.-C. Dong, G.-C. Guo, J.-S. Huang. *Chinese J. Struct. Chem*., **23**, 135 (2004); (d) J. Wang, W. Wang, J. Niu. *J. Mol. Struct*., **873**, 29 (2008); (e) S. Chang, C. Qin, E. Wang, Y. Li, X. Wang. *Inorg. Chem. Commun*., **9**, 727 (2006); (f) J. Sha, J. Peng, H. Liu, J. Chen, A. Tian, B. Dong, P. Zhang. *J. Coord. Chem*., **61**, 1221 (2008).
[5] (a) C.L. Wang, S.X. Liu, C.Y. Sun, L.H. Xie. *J. Coord. Chem*., **61**, 891 (2008); (b) Y.-H. Liu, P.-T. Ma, J.-P. Wang. *J. Coord. Chem*., **61**, 936 (2008); (c) R. Ma. *J. Coord. Chem*., **61**, 1056 (2008); (d) F.-X. Meng, Y.-G. Chen, H.-J. Pang, D.-M. Shi, Y. Sun. *J. Coord. Chem*., **61**, 1513 (2008); (e) J. Wang, F.-B. Li, L.-H. Tian, S.-Y. Cheng. *J. Coord. Chem*., **61**, 2122 (2008); (f) Y. Ding, H. Chen, E. Wang, Y. Ma, X. Wang. *J. Coord. Chem*., **61**, 2347 (2008); (g) Y.-H. Liu, G.-L. Guo, J.-P. Wang. *J. Coord. Chem*., **61**, 2428 (2008); (h) W. Yang, Y. Liu, G. Xue, H. Hu, F. Fu, J. Wang. *J. Coord. Chem*., **61**, 2499 (2008); (i) J. Meng, X. Wang, Y. Ma, E. Wang, X. Xu. *J. Coord. Chem*., **61**, 2853 (2008); (j) M.-X. Li, G.-L. Guo, J.-Y. Niu. *J. Coord. Chem*., **61**, 2896 (2008); (k) H.-B. Liu, Y. Sun, Y.-G. Chen, F.-X. Meng, D.-M. Shi. *J. Coord. Chem*., **61**, 3102 (2008); (l) J. Wang, D. Yang, J. Niu. *J. Coord. Chem*., **61**, 3651 (2008); (m) X. Wang, X. Lu, P. Li, X. Pei, C. Ye. *J. Coord. Chem*., **61**, 3753 (2008); (n) M.-X. Li, G.-L. Guo, J.-Y. Niu. *J. Coord. Chem*., **61**, 3860 (2008); (o) J. Xie. *J. Coord. Chem*., **61**, 3993 (2008).
[6] J.A. Mair. *J. Chem. Soc*., 2364 (1950).
[7] M.T. Pope, G. Varga. *Inorg. Chem*., **5**, 1249 (1966).
[8] F.-X. Ma, Y.-G. Chen, D.-M. Shi. *Acta Cryst. E*, **64**, m672 (2008).
[9] (a) G.M. Sheldrick. *SHELXS*-97, *Program for Crystal Structure Solution*, University of Göttingen (1997); (b) B.G.M. Sheldrick, *SHELXS*-97, *Program for Crystal Structure Refinement*, University of Göttingen (1997).
[10] (a) W. Chen, H.M. Yuan, J.Y. Wang, Z.Y. Liu, J.J. Xu, M. Yang, J.-S. Chen. *J. Am. Chem. Soc*., **125**, 9266 (2003); (b) Z.G. Han, Y.L. Zhao, J. Peng, C.J. Gómez-García. *Inorg. Chem*., **46**, 5453 (2007).
[11] C.J. Gomez-Garcia, C. Gimenez-Saiz, S. Triki. *Inorg. Chem*., **34**, 4139 (1995).
[12] D.H. Brown. *Spectrochim. Acta*, **19**, 585 (1963).
[13] N. Casafi-Pastort, L.C.W. Baker. *J. Am. Chem. Soc*., **114**, 103842 (1992).